HHS Public Access

Author manuscript

Nat Chem Biol. Author manuscript; available in PMC 2013 September 01.

Published in final edited form as:

Nat Chem Biol. 2013 March ; 9(3): 177–183. doi:10.1038/nchembio.1168.

A new structural paradigm in copper resistance in *Streptococcus pneumoniae*

Yue Fu[1,2], **Ho-Ching Tiffany Tsui**[3], **Kevin E. Bruce**[3], **Lok-To Sham**[3], **Khadine A. Higgins**[1], **John P. Lisher**[1,2], **Krystyna M. Kazmierczak**[3], **Michael J. Maroney**[4], **Charles E. Dann III**[1,2], **Malcolm E. Winkler**[2,3], and **David P. Giedroc**[1,2,*]

[1]Department of Chemistry, Indiana University, Bloomington, IN 47405-7102 USA

[2]Interdisciplinary Graduate Program in Biochemistry, Indiana University, Bloomington, IN 47405 USA

[3]Department of Biology, Indiana University, Bloomington, IN 47405 USA

[4]Department of Chemistry, University of Massachusetts, Amherst, MA 01003 USA

Abstract

Copper resistance has emerged as an important virulence determinant of microbial pathogens. In *Streptococcus pneumoniae*, copper resistance is mediated by the copper-responsive repressor CopY, CupA, and CopA, a copper effluxing P_{1B}-type ATPase. We show here that CupA is a novel cell membrane-anchored Cu(I) chaperone, and that a Cu(I)-binding competent, membrane-localized CupA is obligatory for copper resistance. The crystal structures of the soluble domain of CupA (sCupA) and the N-terminal metal binding domain (MBD) of CopA ($CopA^{MBD}$) reveal isostructural cupredoxin-like folds each harboring a binuclear Cu(I) cluster unprecedented in bacterial copper trafficking. NMR studies reveal unidirectional Cu(I) transfer from the low-affinity site on sCupA to the high-affinity site of $CopA^{MBD}$. However, copper binding by $CopA^{MBD}$ is not essential for cellular copper resistance, consistent with a primary role of CupA in cytoplasmic Cu(I) sequestration and/or direct delivery to the transmembrane site of CopA for cellular efflux.

*Address correspondence to David P. Giedroc, Department of Chemistry, 212 S. Hawthorne Dr., Bloomington, IN 47405-7102. giedroc@indiana.edu. Telephone: (812) 856-3178. Fax: (812) 856-5710; giedroc@indiana.edu.

Author contributions

Y.F. carried out all protein purification, Cu(I) binding experiments and NMR studies and solved the crystallographic structures of sCupA and $CopA^{MBD}$, the latter in collaboration C.E.D. III. H.-C-T., K.E.B., L.S, and K.M.K. constructed all *Spn* strains and carried out all cell culture and Western blotting experiments under the direction of M.E.W. K.A.H. prepared samples for XAS and analyzed these spectra in collaboration with M.J.M. and J.P.L. made the ICP-MS measurements on cultures grown by K.E.B. D.P.G. conceived of and directed the study and wrote the manuscript.

Competing financial interests

The authors declare no competing financial interests in the work presented here.

Additional information

Supplementary information is available in the online version of the paper.

Accession codes: Atomic coordinates and structure factors have been deposited to the Protein Data Bank with accession codes sCupA (4F2E) and $CopA^{MBD}$ (4F2F).

Copper (Cu) is an essential transition metal in living organisms that functions as a catalytic cofactor in electron transfer reactions, aerobic respiration, photosynthesis, oxidative stress resistance, and in a number of metabolic enzymes by virtue of its ability to undergo reversible oxidation from Cu(I) to Cu(II)[1]. This crucial characteristic of Cu chemistry also makes Cu highly toxic since Cu(I), like ferrous iron, catalyzes the production of hydroxyl radical (OH•) from endogenous hydrogen peroxide (H_2O_2) in the presence cellular reductants, which is highly damaging to cellular lipids, proteins and nucleic acids[2]. As such, the Cu supply in mammals is tightly regulated.

Cu is also essential for proper development and functioning of the immune system[3]. An established feature of innate immunity to bacterial infection is host control of transition metal availability. This has long been recognized for iron[4], and only recently has control of manganese and zinc availability been linked to the host-pathogen interface[5]. In contrast, emerging evidence suggests that Cu may be used to kill microbial pathogens[6] by inducing oxidative stress or in the absence of oxygen, mediating disassembly of enzyme-bound Fe-S clusters[7]. Cu(I) is also a highly competitive metal ion and will out-compete most other divalent metal ion binding sites in proteins[8]. In *Mycobacterium tuberculosis* and *Staphylococcus aureus*, copper stress is a global stress response that mitigates the effects of thiol oxidation, which disrupts the redox status of the cell[9,10]. *E. coli* and *Salmonella* strains lacking the ability to efflux Cu are more susceptible to Cu toxicity[11,12]. Bacterial pathogens have evolved multiple strategies to quickly mitigate the effects of Cu toxicity with the same mechanisms likely used to maintain the cytoplasmic availability of weakly complexed or "free" Cu to low, near undetectable, levels[6,13–16].

Copper resistance in the Gram-positive respiratory pathogen *Streptococcus pneumoniae* (*Spn*) is mediated by a single operon encoding the Cu(I)-dependent repressor, CopY[17], CupA, of unknown function, and a Cu(I)-effluxing P_{1B}-type ATPase, CopA[18]. Although the intracellular requirement for Cu(I) in *S. pneumoniae* is unknown[19], *S. pneumoniae* contains significant cell-associated copper[20], and adaptation to a high Cu(I) environment may be important for invasive disease. Total Cu(I) is replete in the nasopharynx and in lung tissues and *copA* expression is induced in these tissues in intranasally infected mice[18]. Deletion of *copA* leads to poor kinetics of colonization in the nasopharynx and delayed appearance and reduced bacterial loads in the lung[18]; consistent with this, signature-tagged mutagenesis reveals Δ*cupA* and Δ*copA* strains are attenuated in a murine model of lung infection and pneumonia[21].

Bacterial copper chaperones are thought to function in Cu resistance by sequestering Cu(I) and buffering the metal to a very low level[8,22]. This function is enabled by a high affinity for Cu(I)[23], and/or as articulated in the copper trafficking hypothesis, the ability to donate copper to apo-forms of copper-requiring proteins or to membrane transporters that efflux the metal across the cell membrane[24]. Copper transfer is facilitated by transient and specific protein-protein interactions between often isostructural donor and target proteins via a metal-ligand exchange reaction without dissociation of the metal into bulk solvent[25–27]. *S. pneumoniae* lacks the major characterized class of Cu(I) chaperone ubiquitous in eukaryotes and some bacterial systems, exemplified by *S. cerevisiae* or *Synechocystis* Atx1[27] and *B. subtilis* CopZ[28].

In this report, we show that a structurally novel copper chaperone-copper effluxer pair jointly mediates resistance to copper toxicity in *S. pneumoniae* D39 strain. We show that CupA is a plasma membrane-anchored copper binding protein whose membrane localization and high Cu(I) binding affinity are required for cellular copper resistance. The crystallographic structures of sCupA and $CopA^{MBD}$ reveal a new functional twist on the common cupredoxin fold long associated with iron import, cytochrome oxidase assembly and electron transfer[29–31]. Although we establish that the soluble domain of CupA (sCupA) is capable of transferring bound Cu(I) to N-terminal metal binding domain of CopA ($CopA^{MBD}$) in a thermodynamically favorable and kinetically facile reaction, it is not required for cellular copper resistance under conditions of copper stress. These findings suggest that the primary function of membrane anchored CupA under these conditions is to chelate Cu(I) as soon as it enters the cytoplasm, rather than function as an obligatory chaperone to the MBD of CopA.

RESULTS

Both CupA and CopA localize to the plasma membrane

A transcriptomic analysis of wild-type *S. pneumoniae* D39 and an isogenic markerless deletion strain, Δ*copY*, reveals massive upregulation of the expression of downstream genes *cupA* and *copA* with the expression of virtually no other genes significantly affected upon *copY* deletion (Supplementary Results, Supplementary Fig. 1). This finding, coupled with a previous report of copper-induced expression of *copY-cupA-copA,* reveals that the cellular response to Cu stress is mediated solely by the *cop* operon[18].

Although the core domain of CopA looks to be a prototypical bacterial Cu(I)-effluxing CopA of known structure[32], a ≈100 residue domain that exhibits high sequence similarity to CupA is found at the N-terminus of CopA. Notably, both domains contain four conserved candidate ligands for Cu(I), arranged in a Cys….Cys-x-Met-x-Met (where×is any amino acid) sequence (Supplementary Fig. 2). Furthermore, the N-terminus of CupA is predicted to contain a single transmembrane helix. The high sequence similarity of CupA and the N-terminal region of CopA is a hallmark of a cognate copper chaperone-metal binding domain (MBD) pair found in other bacterial species[33]. *S. pneumoniae* does not encode an Atx1 or a CopZ and a bioinformatics analysis reveals that CupA is nearly always found in genomes that lack a recognizable gene encoding CopZ or Atx1. Furthermore, CupA is widely distributed, perhaps more so than CopZ/Atx1, but clearly clustered in *Lactobacillus* and *Streptococcus* (Supplementary Fig. 3).

All CupAs are predicted to harbor a single transmembrane helix that anchors CupA to the plasma membrane. To test this, we created Δ*cupA* and Δ*copA Spn* D39 deletion strains and tested growth on a rich (BHI) medium under microaerophilic conditions in the presence of 0.2 or 0.5 mM added Cu(II) (Supplementary Table 1). Both strains show a marked growth inhibition phenotype relative to the wild-type strain (Fig. 1a and Supplementary Fig. 4a,b), which can be rescued by ectopic expression of CupA from a heterologous promoter (Fig. 1b). This result rules out any unintended polar effect on the expression of the downstream *copA* gene due to deletion of *cupA*; in fact, the Δ*cupA* strain accumulates CopA protein to high levels (Supplementary Fig. 5b). Strains expressing C-terminally FLAG-tagged CupA or

CopA are characterized by a wild-type growth in the presence of 0.2 or 0.5 mM Cu (Supplementary Fig. 4c,d). In contrast, a strain expressing a D442A CopA, which ablates the catalytic Asp residue in the ATPase domain of CopA (based on an alignment with *Legionella* CopA[32]), is indistinguishable from the Δ*copA* strain (Supplementary Fig. 4d). More importantly, a strain expressing CupA lacking the N-terminal transmembrane domain, Δ(2–28) CupA (denoted hereafter sCupA; Fig. 1c and Supplementary Fig. 5a), is also unable to grow under these conditions. These experiments establish that a C-terminal FLAG-tag does not interfere with CupA or CopA function thus allowing us to determine the subcellular localization of both CopA and CupA using a standard fractionation scheme followed by western blotting with anti-FLAG antibody (Fig. 1d and Supplementary Fig. 6). These data reveal that both full-length CupA and CopA localize exclusively to the plasma membrane in *S. pneumoniae*; furthermore, plasma membrane localization of CupA is required for full copper resistance.

Copper binding by sCupA and CopA^{MBD}

The experiments described above suggest that sCupA and CopA^{MBD} bind Cu(I) directly as a means to effect copper resistance. To test this, we carried out anaerobic titration experiments in which Cu(I) was added to apo-sCupA or apo-CopA^{MBD} in the absence and presence of one of two specific Cu(I) chelators, bathocuprione disulfonate (BCS) (log β2=19.8 for Cu^{I}:BCS_2) or bicinchoninic acid (BCA) (log β2=17.2 for Cu^{I}:BCA_2), thus allowing us to access a range of K_{Cu} between 10^{12} and 10^{19} M^{-1}[34]. A global analysis of two representative titrations at two protein concentrations is shown (Supplementary Figs. 7 and 8) with parameter values compiled in Table 1. Titrations in which apo-sCupA was titrated into a solution of Cu^{I}:BCS_2 or Cu^{I}:BCA_2 returned identical parameter values (Supplementary Fig. 9). These titrations reveal that the stoichiometry of Cu(I) binding in both cases is ≈2 per monomer. sCupA is characterized by stepwise affinity constants (K_{Cu1}, K_{Cu2}) of 7.4×10^{17} M^{-1} and 6.2×10^{14} M^{-1}, compared to 2.1×10^{16} M^{-1} and 2.7×10^{13} M^{-1} for CopA^{MBD} (Table 1). Thus, the putative chaperone sCupA binds Cu(I) 20- to 30-fold more tightly than the putative Cu acceptor CopA^{MBD} to *each of* the high affinity and low affinity sites.

Crystallographic structures of sCupA and CopA^{MBD}

In order to understand the structural basis for the Cu(I) binding stoichiometry, affinity and resistance, we solved the X-ray crystallographic structures of sCupA and CopA^{MBD} to 1.45 Å and 1.50 Å resolution, respectively (Fig. 2a–f and Supplementary Table 3). Each structure reveals an eight-stranded β-barrel harboring a binuclear Cu(I) cluster with a single Cys from the β2-β3 loop (Cys49 in CopA^{MBD} and Cys74 in sCupA) functioning as a bridging ligand to each Cu site, denoted S1 and S2. The S1 Cu site is digonal *bis*-thiolato while the more solvent-exposed S2 site is best described as distorted trigonal planar coordination by the three protein-derived ligands, with a long axial coordination bond to a Cl^{-} anion from solution (or distorted trigonal pyramidal; Supplementary Fig. 10 and Supplementary Table 4). A conserved **Cys**-gly-**Met**-asp/asn-**Met** motif position in the β7-β8 loop in each protein provides three of the four donor atoms to the Cu(I) ions. The Cu-Cu distance is 3.15 Å in each case. Both sCupA and CopA^{MBD} adopt a well-known cupredoxin fold, with Dali *z*-scores ranging from 10–12 for cupredoxins of known structure (Supplementary Fig. 11). However, the metal-ligand disposition (Supplementary Table 4) is completely novel,

evidence that nature has adapted this ancient fold[35] to perform Cu(I) trafficking rather than electron transfer.

Despite adopting identical folds with identical Cu(I) coordination chemistries, sCupA and $CopA^{MBD}$ possess contrasting electrostatic surface potentials around the Cu(I) binding sites, with the sCupA largely negatively charged and the $CopA^{MBD}$ largely positively charged in the vicinity of the Cu(I)-binding sites (Fig. 2g–h). Electrostatic complementarity is an established feature of copper chaperone-MBD pairs, which would allow the Cu(I) chelates of each protein to transiently dock and undergo ligand exchange and Cu transfer, without dissociation of bound Cu(I) into solvent[8,36].

The high and low affinity Cu sites in sCupA and $CopA^{MBD}$

The copper trafficking hypothesis[24] states the copper transfer moves from donor chaperone to target protein with or against a relatively shallow thermodynamic gradient as defined by K_{Cu} measured with purified proteins[37,38]. For sCupA and the CopA MBD, the situation is complicated by the presence of two bound Cu(I) ions in each case, with no insight as to which site defines the high and low affinity Cu(I) sites in each case. We therefore used X-ray absorption spectroscopy (XAS) and NMR spectroscopy to define the sequence of Cu(I) binding, exploiting the fact that the stepwise Cu(I) affinities differ by about ≈1000-fold for both sCupA and $CopA^{MBD}$ (Table 1).

The addition of substoichiometric Cu(I) to sCupA and $CopA^{MBD}$ gives rise to Cu(I) near-edge feature in the XANES spectrum whose intensity is consistent with a low-coordination number complex, either n=2 or n=3 (Fig. 3). For Cu_1 $CopA^{MBD}$, the EXAFS spectrum is best-described by a model corresponding to a digonal *bis*-thiolato (2S) complex or a trigonal 2S, $1Br^-$ complex in NaBr; in NaCl, a three-coordinate 2S-Cl^- fit with a long Cu-Cl^- bond (2.42 Å) is the best fit. These data and accompanying Cu(I)-S^- bond distances (2.18 Å) are consistent with Cu(I) binding to the two S1 site thiolate ligands Cys49 and Cys86 (Supplementary Fig. 12 and Supplementary Table 5). For Cu_1 sCupA, the spectra in both NaBr and NaCl are consistent with an n=3 complex, with a best fit 2S, 1N/O complex, consistent, for example, with recruitment of a solvent molecule into the anticipated 2S (Cys74, Cys111) complex (Supplementary Table 6). As expected, XAS analysis of a Cu_2 sCupA sample in NaBr gives rise to an average Cu(I) coordination environment that is consistent with the crystal structure, including the presence of bound Br^- anion (Supplementary Table 7, Supplementary Fig. 12).

We next examined Cu(I) binding to the apoproteins by monitoring perturbations in the amide chemical shifts of uniformly ^{15}N, ^{13}C-labeled samples of sCupA and $CopA^{MBD}$ upon sequential filling each of the two Cu(I) sites (Supplementary Fig. 13). In each case (but more so in $CopA^{MBD}$) the β3-β4 and β7-β8 metal binding loops in the apoproteins are conformationally exchange broadened indicative of substantial μs-ms dynamics in this region (Fig. 4), as recently found for another apo-cupredoxin involved in electron transfer[39]. Stepwise addition of Cu(I) quenches this line broadening with the addition of the first Cu(I) inducing measurable perturbations beyond these loops and into nearby β-strands, *e.g.*, the β7 strand; addition of the second Cu(I) gives rise to significant perturbations in the metal binding loops only (Fig. 4). These perturbation maps are fully consistent with C49

(CopA^{MBD}) and C74 (sCupA) functioning as a bridging ligand since filling of both S1 and S2 Cu sites in each induces backbone perturbations in both β3-β4 and β7-β8 loops.

Although the Cu_1 and Cu_2 states of both sCupA and CopA^{MBD} are readily distinguished from one another (Supplementary Fig. 13) they cannot be used to assign the high- and low-affinity sites. We therefore assigned the methionine ^{13}Cε–Hε groups of both sCupA and CopA^{MBD} by ^{13}C-edited NOESY spectroscopy, with direct Met-Cu(I) coordination expected to induce a strong downfield shift of the ^{13}Cε chemical shift as revealed by a ^{1}H, ^{13}C-HSQC spectrum (Fig. 3c)[40]. Consistent with XAS, only upon addition of the second mol•equiv Cu(I) is there a strong downfield shift of the ^{13}Cε-^{1}Hε methyl crosspeaks of M88 and M90 of CopA^{MBD} indicative of direct ligation (Fig. 3c). For sCupA, addition of the first mol•equiv of Cu(I) results in a slight *upfield* shift of the M116 ^{13}Cε–Hε with few other changes in the spectrum; only upon addition of the second mol•equiv of Cu(I) is there a strong downfield shift of the methyl resonances of M113 and M115. Inspection of the sCupA structure reveals that M116 is quite close to the S1 Cu ion, and thus reports on filling the digonal *bis*-thiolato S1 site (Fig. 3d). We conclude that the high affinity Cu(I) site on both CopA^{MBD} and sCupA is the *bis*-thiolato S1 site, with the more solvent-exposed Met-rich S2 site the low affinity Cu(I) site in each protein.

NMR detection of facile Cu transfer from sCupA to CopA^{MBD}

We next determined if Cu(I) bound to the putative donor sCupA could be transferred to acceptor CopA^{MBD}, taking advantage of the distinct spectroscopic signatures of Cu(I) bound to each of the two Cu(I) sites (Fig. 3c,d). We performed this experiment using an NMR-based strategy[31] by mixing ^{13}C,^{15}N-sCupA with unlabeled CopA^{MBD} or unlabeled sCupA with ^{13}C,^{15}N-CopA^{MBD}, with sCupA loaded with two mol•equiv of Cu(I) as copper donor. When unlabeled apo-CopA^{MBD} is mixed with stoichiometeric Cu_2 ^{13}C,^{15}N-sCupA, one Cu(I) is lost, specifically from the low-affinity Met-rich S2 site as evidenced by a return of the ^{13}Cε-^{1}Hε crosspeaks of M113 and M115 to their positions in Cu_1 sCupA (Fig. 3d); the same is evident on inspection of the ^{1}H,^{15}N-HSQC spectrum of sCupA, with the Cu_2 resonances lost, and concomitant superposition of the crosspeaks associated with *bona fide* Cu_1 sCupA and those that results when Cu_2 sCupA is mixed with apo-CopA^{MBD} (Fig. 3f). There is no trace of apo-sCupA in these spectra. Monitoring the same reaction with excess (2:1) unlabeled Cu-saturated sCupA and ^{13}C,^{15}N-apo-CopA^{MBD} reveals formation of only the *bona fide* Cu_1 CopA^{MBD} with the S1 sites filled (Fig. 3c), with no evidence of the Cu_2 or apo-MBD in these mixtures (Fig. 3e). Thus, even in the presence of excess Cu bound to sCupA, only the high affinity S1 site on the CopA^{MDB} is capable of accepting the Cu(I) from sCupA, and that Cu(I) is donated from the more solvent-exposed lower affinity S2 site on sCupA.

The reverse experiment was also done in which stoichiometric ^{13}C,^{15}N-labeled Cu_1 CopA^{MBD} was mixed with unlabeled apo-sCupA. There is no change in the spectrum (Supplementary Fig. 14), thus revealing that despite the higher affinity, the S1 site on sCupA is unable to strip the MDB of its bound Cu(I) under these conditions. Efficient Cu(I) transfer is therefore preferentially unidirectional, but may depend on the molar ratio of CupA and CopA in the membrane.

Cu resistance requires Cu binding by CupA but not CopA^{MBD}

In order to further understand the essentiality of CupA for copper resistance we characterized *cupA* allelic replacement strains using our structure as a guide (Fig. 2). Mutant *cupA* strains include M113A/M115A (*cupA*(2A)), which abrogates binding to the S2 site only; a triple Cu-coordinating β7-β8 loop mutant (C111A/M113A/M115A) designated (*cupA*(3A)); a single bridging ligand substitution of C74 (*cupA*(C74S)); and a quadruple mutant in which all metal ligands are substituted with nonliganding residues (*cupA*(C74S, 3A)). C74S sCupA binds a single mol•equiv of Cu(I) with a low affinity ($K_{Cu} \approx 10^{12}$ M^{-1}) but adopts a fold identical to that of wild-type sCupA with only local structural perturbations near the substitution (Supplementary Fig. 15).

In the absence of added copper, all *cupA* metal-liganding mutant strains grow similarly to the wild-type (WT) strain (Fig. 5a). However, in the presence of 0.2 mM Cu(II), growth of the *cupA*(3A) strain is inhibited but viable, while the *cupA*(2A), *cupA*(C74S) and *cupA*(C74S,3A) strains all fail to grow significantly (Fig. 5b), despite the fact that these CupAs accumulate to a level greater than that of wild-type CupA (Supplementary Fig. 5a). At 0.5 mM Cu(II), none of the mutant *cupA* strains is able to grow (Supplementary Fig. 16b). In fact, the behavior of the *cupA*(C74S) strain is indistinguishable from a *copA*(D442A) strain expressing a catalytically inactive CopA (Fig. 5c). Interestingly, western blotting reveals that CopA accumulates to very high levels in both strains, as well as in the Δ*cupA* strain (Supplementary Fig. 5b). Analysis of the total cell-associated metal content of these strains by ICP-MS reveals a substantial increase in total cellular Cu, which reaches a level ≈5-fold higher than WT cells 3 h after addition of 0.2 mM Cu in the Δ*cupA* and *cupA*(C74S) strains (Supplementary Table 8).

In contrast, when a substitution that is analogous to C74S in CupA is introduced into the CopA^{MBD} in the *copA* gene (*copA*(C49S)), copper resistance is unaffected at both 0.2 mM (Fig. 5c) and 0.5 mM Cu(II) (Supplementary Fig. 16c). Consistent with this, FLAG-tagged C49S CopA accumulates to a level similar to that of wild-type CopA rather than to that of Cu-sensitive mutants (Supplementary Fig. 5b). These experiments thus establish that a major function of CupA in copper stress resistance is likely not to chaperone Cu(I) to the CopA^{MBD} but instead is required for direct copper delivery to the transmembrane Cu(I) binding sites in CopA for efflux and/or to sequester Cu(I) during copper stress in an effort to mitigate the effects of cellular Cu toxicity.

DISCUSSION

In this work, we define a new structural paradigm for copper trafficking and resistance characterized in the Gram-positive respiratory pathogen *S. pneumoniae*. Soluble CupA and CopA^{MBD} are isostructural and of opposite electrostatic surface potentials, and each harbors a binuclear Cu(I) cluster in the context of a novel architecture not previously observed in bacterial copper trafficking. The Cu(I) binding affinities of sCupA and CopA^{MBD} differ significantly from one another, and although sCupA binds Cu(I) more tightly overall than CopA^{MBD}, copper transfer is preferentially down a thermodynamic gradient, from the low affinity S2 site of sCupA to the high affinity S1 site of CopA^{MBD}, as found in many other Cu(I) chaperone systems[23,37,38]. CupA therefore satisfies all established criteria for

designation as a copper chaperone[33], but is the first one known to be inserted into the plasma membrane which itself is obligatory for copper resistance.

This is the first instance to our knowledge where biological studies establish that deletion or functional inactivation of the copper chaperone reduces copper resistance to a level identical to deletion or inactivation of the copper transporter itself. This requirement of the CupA chaperone in Cu resistance in *Spn* was missed in the previous report, which suggested that a *Spn* strain encoding a translationally terminated *cupA* gene gave rise only to a more modest copper sensitivity phenotype[18]. We show here that CupA protein levels in all *cupA* missense strains that express CupA with diminished Cu(I)-binding affinities accumulate to a level greater than that in a wild-type background. A hyperaccumulation of both CupA and CopA in these cells may be reporting on hypersensitivity or continued derepression of CopY-mediated transcription of the *cop* operon in a failed effort to resist the effects of increased cytoplasmic copper.

Although Cu transfer from the S2 site of CupA to the S1 site of $CopA^{MBD}$ occurs spontaneously, we suggest that this may occur only under non-stressed or "housekeeping" conditions since it is not strongly relevant to the cellular Cu toxicity response. In fact, recent studies[32,41] support a model in which the N-terminal MBD (not visualized in the crystallographic structure of *Legionella* CopA) plays a regulatory role. Here, the MBD is thought to dock against the actuator domain (Supplementary Fig. 17) and inhibit ATP hydrolysis in the absence of Cu(I); metal binding by the MBD then disrupts this interaction, allosterically activating ATP hydrolysis and Cu(I) transport. It is known that the cytoplasmic copper chaperone Atx1 can deliver Cu(I) to either the N-terminal MBD, which is not on-pathway for copper transfer, or the transmembrane site directly[42], the latter hypothesized to occur via docking to the positively charged platform region that surrounds the putative entry site for Cu transfer[32]. Thus, the negative electrostatic surface potential of sCupA is complementary to both the MBD and the platform region of CopA, and may facilitate transient docking and direct Cu delivery to either site (Supplementary Fig. 17).

Our data are consistent with recent experiments in *Synechocystis* and in *Listeria monocytogenes* which suggest that a primary role of the copper chaperone is to buffer free Cu(I) to a very low level, thus preventing what is a highly competitive, thiophilic metal from binding indiscriminately to other cellular targets[8,22]. There is little known about the intracellular cuproproteome of *S. pneumoniae* and it is unknown how copper enters the cell[15,43,44]. In addition, there are as yet no known targets of CupA chaperone function, outside of CopA characterized here. Other functional roles for CupA are possible, particularly so given that the metallochaperone for the Cu_A subunit of a bacterial cytochrome *c* oxidase is itself a membrane-anchored cupredoxin-fold protein that binds a single Cu(I) ion[30,31]. However, CupA is not performing this role in *S. pneumoniae* since it lacks cytochrome oxidase and an electron transport chain[45].

We propose that the primary role of CupA in *S. pneumoniae* is to chelate Cu(I) as soon as it enters the cytoplasm, near the plasma membrane, and via two-dimensional diffusion in the membrane, interacts with the effluxer and delivers Cu(I) directly to the core of CopA for Cu(I) efflux. The significant negative charge associated with the inner plasma membrane

may aid in this process by holding the positively charged Cu(I) cation near the membrane for subsequent binding by CupA. Any Cu(I) that becomes cytoplasmic is then sensed by CopY, which binds Cu(I) and induces upregulation of CupA and CopA in an effort to reduce intracellular Cu content via efflux. Such strict control of bioavailable Cu(I) in the cytoplasm might be dictated by the unique physiology of *S. pneumoniae* relative to those bacteria previously studied. *Spn* is an aerotolerant anaerobe that generates millimolar levels of H_2O_2 used to kill other bacteria in the community[45]. As such, *Spn* may go to great lengths to resist the potential collateral damage of endogenous H_2O_2[46]. These studies identify potential new targets for the development of antibiotics to combat emerging multidrug resistant strains of *S. pneumoniae* and related pathogenic streptococci[47].

ONLINE METHODS

Bacterial strains and growth conditions

Streptococcus pneumoniae serotype 2 strain D39 and its derivatives were used in this study[48]. Strains containing antibiotic markers were constructed by transforming linear DNA amplicons synthesized by overlapping fusion PCR into competent pneumococcal cells[49]. Strains containing markerless *copY*, *cupA* or *copA* and respective FLAG-tagged alleles in native gene loci (Supplementary Table 1) were generated using the P_c-[*kan*^{R}-*rpsL*$^+$] (Janus cassette) allele replacement method[49]. Δ*copY* and Δ*copA* alleles in IU3566 (D39 Δ*copY*) and IU5975 (D39 Δ*copA*) strains were constructed by deletion of the gene sequences except for the 60 bp at the 5' and 3' end. Δ*cupA* allele in IU5971 (D39 Δ*cupA*) was constructed by deletion of *cupA* gene sequence except for the 5' 42 bp and 3' 60 bp. All constructs were confirmed by DNA sequencing of the amplicon region used for transformation. Strains were grown on plates containing Trypticase Soy Agar II (Modified) (Becton-Dickinson; BD) and 5% (v/v) defibrinated sheep blood (TSAII BA), and incubated at 37 °C in an atmosphere of 5% CO_2. For antibiotic selections, TSAII BA plates were supplemented with 250 μg kanamycin per mL or 250 μg streptomycin per mL. For liquid cultures, strains were cultured statically in BD Brain-Heart Infusion (BHI) broth at 37 °C in an atmosphere of 5% CO_2. To obtain growth curves, overnight cultures were obtained from frozen stock inoculums into 3 mL of BHI broth in 17-mm-diameter polystyrene plastic tubes and serially diluted over five tubes. Overnight cultures still in log-phase growth were diluted to OD_{620} of 0.002 in BHI with or without 0.2 or 0.5 mM $CuSO_4$. Growth was monitored by OD_{620} using a Spectronic 20 Genesys spectrophotometer.

Cell fractionation and subcellular localization of CupA and CopA in *S. pneumoniae* D39

Biochemical fractionation of pneumococcal cells was performed as described[50] with strains IU6041 (*cupA*-(C)-FLAG) and IU6044 (*copA*-(C)-FLAG) in BHI supplemented with 0.3 mM $CuSO_4$.

Western blotting to quantitate cellular expression levels of CupA and CopA in various *cupA* or *copA* mutants

Whole cell lysates were prepared from the indicated strains using the FastPrep method on cell cultures grown overnight in BHI and then diluted to 0.0035 (*cupA* (C)-FLAG, WT, *copA* (C)-FLAG and *copA* (C49S)-(C)-FLAG) or 0.005 (all other mutant strains) in 30 mL

BHI, and allowed to grow to an OD_{620} of 0.04 (*cupA* (C)-FLAG, WT, *copA* (C)-FLAG and *copA* (C49S)-(C)-FLAG) or 0.06 (all other strains) or ≈3 doublings, at which time $CuSO_4$ was added to a final concentration of 0.2 mM. 2.5 h after addition of Cu, at an OD_{620} of ≈0.25 for *cupA*-FLAG strains (≈2 doublings for Cu-sensitive mutant alleles and ≈3 doublings for WT and *cupA* (C)-FLAG) and at an OD_{620} of ≈0.5 for *cop*A-FLAG strains (≈2 doublings for Cu-sensitive mutant alleles and ≈3 doublings for WT, *copA* (C)-FLAG and *copA* (C49S)-(C)-FLAG), cells were centrifuged at 14,500 × *g* for 5 min at 4 °C. Supernatants were removed and pellets were placed on ice and suspended in 1.0 mL of cold 20 mM Tris pH 7.0 and 8 μL of protease inhibitor cocktail set III (Calbiochem) and transferred to chilled Lysing Matrix B tubes (MP Biomedicals). Matrix tubes were secured in a 24 × 2 mL-tube adapter in a FastPrep-24 instrument (MP Biomedicals) stored at 4 °C. Cells were disrupted by three consecutive runs of 40 sec each at a speed setting = 6.0 m/s. Lysed cell mixtures were placed on ice and centrifuged at 10,000 × *g* for 1 min at 4 °C. 100 μL of supernatant was transferred to a tube containing 100 μL of cold 2× Laemmli sample buffer (containing 5% (vol/vol) of freshly added β-mercaptoethanol), boiled for 5 min and placed on ice. Gel loading volumes were calculated to adjust for the slightly different cell culture densities. Visualization and relative quantitation of FLAG-tagged proteins were achieved with Western blotting with primary anti-FLAG polyclonal antibody (Sigma, F7425) and an IVIS imaging system[48].

Bioinformatics analysis

The sequences of CupA and *B. subtilis* CopZ and *Synechocystis* (sc) Atx1 were used as query in a pBLAST analysis against non-redundant protein sequence database of all bacterial genomes. Criteria for designation as a CupA, CopZ and scAtx1 are shown in Supplementary Fig. 3.

ICP-MS analysis

1.5 mL aliquots of *S. pneumoniae* strains were centrifuged and washed once with BHI containing 1 mM nitrilotriacetic acid (Aldrich), then twice with PBS that had been treated overnight with Chelex-100 (Biorad) according to the manufacturer's protocol. The cell pellets were dried overnight, 400 μL of 2.5% v/v nitric acid (Ultrapure, Sigma- Aldrich) containing 0.1% v/v Triton-X 100 was added to solubilize the cell pellets, and were lysed for 10 min at 95 °C with shaking at 500 rpm followed by vigorous vortexing for 20 s. 200 μL of the lysed cell solution (equivalent to 0.75 mL total cell culture) was added to 2.8 mL of 2.5% v/v nitric acid for ICP-MS analysis. Analyses were performed using a Perkin Elmer ELAN DRCII ICP-MS essentially as described earlier[20]. Germanium at 50 ppb was added as an internal standard using an EzyFit glass mixing chamber. Metal concentration per mg protein were determined in the following way. ICP-MS gave [metal] in μg/L * 0.003 L sample equals total μg metal in 0.75 mL of cell culture. The μg metal * 1000 * 2 gave the ng metal in the original 1.5 mL of culture. Protein samples were resuspended in 100 μL buffer and concentrations were determined in mg/mL using a Bradford assay (Biorad). Total protein in 1.5 mL was calculated multiplying by 0.1 to correct for the resuspension volume. The final copper concentration as expressed by ng metal/mg protein determined by dividing those two values (ng/1.5 mL)/(mg/1.5 mL) = ng/mg protein.

Construction of overexpression plasmids and protein purification

The pHis-parallel plasmid was used to subclone sCupA (residues 29–123 of the 123-residue CupA) and the $CopA^{MBD}$ (residues 1–99 of CopA). These constructs, following TEV protease cleavage, yield a non-native Gly-Ala-Met N-terminal sequence for sCupA (denoted residues 26–28 in the structure) and a single non-native N-terminal Gly in the case of $CopA^{MBD}$(denoted Gly0). *E. coli* BL21 (DE3) competent cells were transformed with the resultant plasmids. For unlabeled proteins, overnight cultures were inoculated into LB containing 100 μg/mL ampicillin. For the $^{15}N/^{13}C$ labeled proteins, overnight cultures were inoculated into M9 minimal media (pH 7.4) containing 100 μg/mL ampicillin, supplemented with $^{15}NH_4Cl$ (1 g/L) (Cambridge Isotope Laboratories) and [$^{13}C_6$]-D-glucose (2.5 g/L) (Cambridge Isotope Laboratories). For both media, the cells were grown at 37 °C to OD_{600} = 0.6 with isopropyl β-*d*-thiogalactopyranoside (IPTG) added to a final concentration of 0.4 mM and cultures continued at 16 °C for 20 h. The cells were harvested by centrifugation and kept at –80 °C. All buffers in the purification were placed under argon using a Schlenk line immediately before use. For lysis, cells were resuspended in buffer R (25 mM Tris, pH 8.0, 200 mM NaCl, 5 mM TCEP). The resuspended cells were lysed by a sonic dismembranator (Fisher). The recombinant proteins were purified using HisTrap FF columns (GE Healthcare) using a gradient of imidazole from 10 mM to 300 mM in buffer R. The appropriate fractions were pooled and subjected to TEV protease cleavage at for 16 °C for 36 h. The proteins were further purified using HisTrap FF columns (GE Healthcare) and Superdex 75 16/60 column (GE Healthcare). The purity of the proteins was estimated to be >95 % as judged by SDS-PAGE. Protein concentration was determined by A_{280} with an extinction coefficient of 4595 $M^{-1}cm^{-1}$. The number of reduced thiols was 1.9 for sCupA and 1.7 for $CopA^{MBD}$ (2.0 expected). Mutants of sCupA and $CopA^{MBD}$ were generated using a standard site-directed mutagenesis strategy (Stratagene), and mutant proteins purified as described above.

Cu(I) Binding Affinity Measurements

Bathocuproine disulfonate (BCS) and bicinchoninic acid (BCA) were used for Cu(I) binding affinity determination of sCupA and $CopA^{MBD}$ by direct Cu(I) titration into a mixture of chelator and apoprotien essentially as described previously or titration of apoprotein into a chelator-copper complex[34]. Apoproteins were buffer exchanged into degassed buffer B (25 mM HEPES, pH 7.0, 200 mM NaCl) in an anaerobic chamber. The Cu(I) stock was prepared by taking the supernatant following anaerobic dissolution of solid CuCl into fully degassed buffer B (25 mM HEPES, pH 7.0, 200 mM NaCl). The concentration of Cu(I) stock was determined by atomic absorption spectroscopy (Perkin Elmer AAS-400) with a typical stock concentration of ≈10 mM. For direct Cu(I) titrations, the final solution to be titrated contained 20 or 30 μM sCupA or $CopA^{MBD}$ and 30 or 40 μM BCA (BCS) in Buffer B. Each 120 μL aliquot of titration solution was mixed with increasing Cu(I) titrant. For apoprotein titrations, a concentrated stock solution of the apo-sCupA was titrated into a solution containing 27–40 μM Cu(I) and 80–162 μM BCS or 25–35 μM Cu(I) and 170–285 μM BCA. Under these conditions all the Cu(I) is bound as a $Cu:BCS_2$ or $Cu:BCA_2$ chelate, respectively, prior to addition of apo-CupA.

In both experiments, the optical spectra of BCA or BCS were recorded from 200 nm to 900 nm. Corrected spectra were obtained by subtracting apo-sCupA (or $CopA^{MBD}$) spectrum from each Cu(I)-addition spectrum and then corrected for dilution. A_{483} was used to determine the concentration of Cu^{I}:BCS_2 complex with an extinction coefficient of 13500 $M^{-1}cm^{-1}$. A_{562} was used to determine the concentration of Cu^{I}:BCA_2 complex with an extinction coefficient of 7700 $M^{-1}cm^{-1}$. All the data were fitted to the appropriate competition model using Dynafit[51].

Crystallization and crystal structure determination

Apo protein (sCupA or $CopA^{MBD}$) was first buffer exchanged to fully degassed buffer A (25 mM Tris, pH 8.0, 200 mM NaCl) in an anaerobic glove box. A ≈10 mM Cu(I) stock solution was prepared by taking the supernatant from dissolution of solid CuCl into fully degassed buffer B (25 mM HEPES, pH 7.0, 200 mM NaCl) with the concentration of Cu determined by atomic absorption spectroscopy. Cu(I) loaded proteins were prepared by mixing apo protein with a freshly prepared Cu(I) stock in the glove box at a 1:2 protein:Cu molar ratio. Cu(I)-sCupA was crystallized by hanging drop vapor diffusion at 20 °C against a well buffer of 30 % (w/v) PEG 3350, 0.1 M sodium citrate tribasic dihydrate pH 5.0 and Big CHAP Deoxy. The cryosolvent was prepared using 35 % (w/v) polyethylene glycerol 3350 in the well solution. Cu(I)-$CopA^{MBD}$ was crystallized by hanging drop vapor diffusion at 20 °C against a well buffer of 28 % (w/v) polyethylene glycerol monomethyl ether 2000, 0.1 M Bis-Tris pH 6.5. The cryosolvent was prepared by using 35 % (w/v) polyethylene glycerol monomethyl ether 2000 in the well solution. For $CopA^{MBD}$, diffraction data for the native data set were collected at −160 °C on an R-AXIS IV+ detector at Indiana University, Bloomington. The space group of the crystal was $P2_12_12_1$ with one monomer in the asymmetric unit. All data were processed with HKL2000 and diffraction data for the initial phase determination collected on ALS 4.2.2 (Advanced Light Source, Lawrence Berkeley National Laboratory). Initial phases for the structure of $CopA^{MBD}$ were determined by single-wavelength anomalous dispersion (SAD) techniques from a dataset collected on beamline 4.2.2 at the Advanced Light Source with Cu(I) providing an anomalous signal for phasing. The structure of $CopA^{MBD}$ was solved and auto-built with PHENIX[52]. Two Cu(I) atoms were found in the structure. Iterative rounds of model building and refinement were carried out in Coot[53] and PHENIX[52], respectively. Ramachandran statistics were 98% of the residues in the allowed region, 2% generously allowed, and 0% disallowed. For sCupA, diffraction data were collected at Indiana University, Bloomington, as described above. The space group of the crystal was $P2_12_12$ with one monomer in the asymmetric unit. Following processing with HKL2000, initial phases were calculated using a truncated model of $CopA^{MBD}$ as a molecular replacement search model in PHENIX[52] with the structure refined as described above for $CopA^{MBD}$. Ramachandran statistics for sCupA were 100% of the residues in the allowed region with 0% in the generously allowed and disallowed regions. All structure related figures were prepared using PyMOL (Delano Scientific).

NMR methods

Typical NMR sample solution conditions were 300–600 μM ^{15}N, ^{13}C-labeled sCupA or $CopA^{MBD}$, pH 6.0, 50 mM sodium phosphate, 50 mM NaCl, 0.02% (w/v) NaN_3 and 10% (v/v) ^2H_2O, 25 °C. All NMR samples were prepared in an anaerobic glove box. Apo state

samples (sCupA and $CopA^{MBD}$) were prepared with 5 mM TCEP. Cu_1 sCupA samples contained 0.9 mol equiv of Cu(I) and Cu_2 sCupA samples contained 1.9 mol equiv of Cu(I). Cu_1 $CopA^{MBD}$ samples contained 0.8 mol equiv of Cu(I) and Cu_2 $CopA^{MBD}$ samples contain 1.8 mol equiv of Cu(I). NMR spectra were acquired with a Varian DDR 800 MHz spectrometer equipped with a cryogenic probe at the Indiana University METACyt Biomolecular NMR laboratory. The NMR spectra were processed using NMRPipe[54] and analyzed using Sparky (T. D. Goddard and D. G. Kneller, SPARKY 3, University of California, San Francisco). Chemical shifts are referenced relative to internal 2,2-dimethyl-2-silapentene-5-sulfonic acid (DSS).

Sequential backbone resonance assignments of all six states (apo, Cu_1 and Cu_2 states of sCupA and $CopA^{MBD}$) were obtained using ^{1}H-^{15}N heteronuclear single quantum coherence (HSQC), HADAMAC-2[55], and triple resonance CBCA(CO)NH, CBCANH, HNCO and Best-HNCA[56] spectra. The automatic backbone assignment server PINE was employed to aid in obtaining assignments. Methionine $^{13}CH_3$ resonance assignments of Cu_2 sCupA were obtained from a ^{1}H, ^{13}C HSQC experiment using HCCH-TOCSY, HCCH-COSY and ^{13}C-edited NOESY-HSQC experiments. The NOESY experiments were conducted using standard pulse sequences from the Varian Biopack with τ_m=100 ms. 1024×200×70 data points were acquired for the ^{13}C -edited NOESY-HSQC experiment.

X-ray Absorption Spectroscopy (XAS)

sCupA and MBD were concentrated to 2 mM and 1.2 mM respectively in 25 mM Hepes (pH 7.0) and 200 mM NaCl or NaBr. 0.8 molar equivalent of CuCl or CuBr was added to both MBD and CupA anaerobically. 30 μL of each sample was syringed into polycarbonate XAS holders that were wrapped in kapton tape and frozen in liquid nitrogen. XAS data were collected at beamline 7–3 at the Stanford Synchrotron Radiation Laboratory (SSRL). Data were collected at 10 K using a liquid helium cryostat (Oxford Instruments). The ring conditions were 3GeV and 80–100mA. Beamline optics consisted of a Si(220) double-crystal monochromator and two rhodium-coated mirrors. X-ray fluorescence was collected using a 30-element Ge detector (Canberra). Scattering was minimized using Soller slits and placing a Z-1 filter between the sample chamber and the detector.

The $Cu_{1.8}$ sCupA sample was prepared by adding 1.8 molar equivalents of CuBr to 3 mM sCupA in 25 mM Hepes (pH 7.0) and 200 mM NaBr and concentrated to 3 mM under anaerobic conditions. 60 μL was syringed into a polycarbonate XAS holder wrapped in kapton tape and frozen in liquid nitrogen. The data were collected at beam line X3b at the National Synchrotron Light Source (NSLS), Brookhaven National Laboratories. The samples were loaded into an aluminum sample holder, which was cooled to ~50 K using a He displex cryostat. Data were collected under ring conditions of 2.8 GeV and 120–300 mA using a sagitally focusing Si(111) double-crystal monochromator. Harmonic rejection was accomplished with a Ni-coated focusing mirror. X-ray fluorescence was collected using a 30-element Ge detector (Canberra). Scattering was minimized by placing a Z-1 filter between the sample chamber and the detector. For all samples, XANES was collected from ± 200 eV relative to the metal edge. The X-ray energy for the Cu metal K_α-edge was

internally calibrated to the first inflection point, 8980.3 eV. EXAFS was collected to 15 *k* above the edge energy (E_o).

XAS Data Reduction and Analysis

The XAS data shown (*vide infra*) are the average of 8 scans. XAS data was analyzed using SixPack[57]. The SixPack fitting software builds on the ifeffit engine[58,59]. Each data set was background-corrected and normalized. For EXAFS analysis each data set was converted to *k*-space using the relationship

$$k=\left[2m_e(E-E_o)/\hbar^2\right]^{1/2}$$

where m_e is the mass of the electron, $\hbar$ is Plank's constant divided by 2π, and E_o is the threshold energy of the absorption edge. The threshold energy chosen for copper is 8990 eV[60]. The best fits for the data sets were obtained using a Fourier-transform of the data was produced using data over the range *k* = 2–14 Å^{-1} ($Cu_{0.8}$ sCupA and $Cu_{0.8}$ $CopA^{MBD}$) or *k* = 2–12.5 Å^{-1} ($Cu_{1.8}$ sCupA) where the upper limit was determined by the signal:noise ratio. Scattering parameters were generated using FEFF 8[59]. The first coordination sphere was determined by setting the number of scattering atoms in each shell to integer values and systematically varying the combination of N/O and S-donors (Supplementary Tables 5–7). To compare different models of the same data set, ifeffit utilizes three goodness of fit parameters: χ^2, reduced χ^2, and the R-factor. χ^2 is given by equation 1, where N_{idp} is the number of independent data points, N_{ε^2} is the number of uncertainties to minimize, Re(f_i) is the real part of the EXAFS function, and Im(f_i) is the imaginary part of the EXAFS fitting function (eq. 1)

$$\chi^2=\frac{N_{idp}}{N_{\varepsilon^2}}\sum_{i=1}^{N}\left\{[\mathrm{Re}(f_i)]^2+[\mathrm{Im}(f_i)]^2\right\} \quad (1)$$

Reduced $\chi^2 = \chi^2/(N_{ind} - N_{\mathrm{var}\,ys})$ where N_{varys} is the number of refining parameters and represents the degrees of freedom in the fit. Additionally Ifeffit calculates the R-factor for the fit, which is given by equation 2, and is scaled to the magnitude of the data making it proportional to χ^2 (eq. 2)

$$R=\frac{\sum_{i=1}^{N}\left\{[\mathrm{Re}(f_i)]^2+[\mathrm{Im}(f_i)]^2\right\}}{\sum_{i=1}^{N}\left\{[\mathrm{Re}(\tilde{x}data_i)]^2+[\mathrm{Im}(\tilde{x}data_i)]^2\right\}} \quad (2)$$

In comparing different models, the R-factor and reduced χ^2 parameter were used to determine which model was the best fit for the data. The R-factor will always generally improve with an increasing number of adjustable parameters, while reduced χ^2 will go through a minimum and then increase, indicating that the model is over fitting the data.

Supplementary Material

Refer to Web version on PubMed Central for supplementary material.

Acknowledgements

The authors gratefully acknowledge support from the National Institutes of Health (GM042569 to D.P.G., GM094472 to C.E.D. III, AI1095814 to M.E.W. and GM069696 to M.J.M.), the Lilly Endowment (to M.E.W.) and an Indiana University Quantitative and Chemical Biology Training Fellowship (to J.P.L.). We thank Lauren Christiansen for assistance in strain construction, members of the Giedroc laboratory for help in acquiring the NMR data, and Heidi Hu and Nitai Girifrom of the Maroney laboratory for XAS data collection. Crystallographic data collection at the Advanced Light Source at the Lawrence Berkeley National Laboratory is supported by the US Department of Energy and Indiana University. The SSRL Structural Molecular Biology Program is supported by the Department of Energy, Office of Biological and Environmental Research, and by the National Institutes of Health National Center for Research Resources, Biomedical Technology Program. XAS data collected at the National Synchrotron Light Source at Brookhaven National Laboratory was supported by the U.S. Department of Energy, Division of Materials Sciences and Division of Chemical Sciences. Beam line X3B at NSLS is supported by the Center for Synchrotron Biosciences grant, P30-EB-009998, from the National Institute of Biomedical Imaging and Bioengineering.

References

1. Pena MM, Lee J, Thiele DJ. A delicate balance: homeostatic control of copper uptake and distribution. J. Nutr. 1999; 129:1251–1260. [PubMed: 10395584]
2. Halliwell B, Gutteridge JM. The importance of free radicals and catalytic metal ions in human diseases. Mol. Aspects Med. 1985; 8:89–193. [PubMed: 3908871]
3. Percival SS. Copper and immunity. Am. J. Clin. Nutr. 1998; 67:1064S–1068S. [PubMed: 9587153]
4. Braun V, Hantke K. Recent insights into iron import by bacteria. Curr. Opin. Chem. Biol. 2011; 15:328–334. [PubMed: 21277822]
5. Corbin BD, Seeley EH, Raab A, Feldmann J, Miller MR, Torres VJ, et al. Metal chelation and inhibition of bacterial growth in tissue abscesses. Science. 2008; 319:962–965. [PubMed: 18276893]
6. Samanovic MI, Ding C, Thiele DJ, Darwin KH. Copper in microbial pathogenesis: meddling with the metal. Cell Host Microbe. 2012; 11:106–115. [PubMed: 22341460]
7. Macomber L, Imlay JA. The iron-sulfur clusters of dehydratases are primary intracellular targets of copper toxicity. Proc. Natl. Acad. Sci. USA. 2009; 106:8344–8349. [PubMed: 19416816]
8. Tottey S, et al. Cyanobacterial metallochaperone inhibits deleterious side reactions of copper. Proc. Natl. Acad. Sci. USA. 2012; 109:95–100. [PubMed: 22198771]
9. Baker J, Sitthisak S, Sengupta M, Johnson M, Jayaswal RK, Morrissey JA. Copper stress induces a global stress response in *Staphylococcus aureus* and represses *sae* and *agr* expression and biofilm formation. Appl. Environ. Microbiol. 2010; 76:150–160. [PubMed: 19880638]
10. Ward SK, Hoye EA, Talaat AM. The global responses of *Mycobacterium tuberculosis* to physiological levels of copper. J. Bacteriol. 2008; 190:2939–2946. [PubMed: 18263720]
11. White C, Lee J, Kambe T, Fritsche K, Petris MJ. A role for the ATP7A copper-transporting ATPase in macrophage bactericidal activity. J. Biol. Chem. 2009; 284:33949–33956. [PubMed: 19808669]
12. Osman D, Waldron KJ, Denton H, Taylor CM, Grant AJ, Mastroeni P, et al. Copper homeostasis in *Salmonella* is atypical and copper-CueP is a major periplasmic metal complex. J. Biol. Chem. 2010; 285:25259–25268. [PubMed: 20534583]
13. Gold B, Deng H, Bryk R, Vargas D, Eliezer D, Roberts J, et al. Identification of a copper-binding metallothionein in pathogenic mycobacteria. Nat. Chem. Biol. 2008; 4:609–616. [PubMed: 18724363]
14. Festa RA, Jones MB, Butler-Wu S, Sinsimer D, Gerads R, Bishai WR, et al. A novel copper-responsive regulon in *Mycobacterium tuberculosis*. Mol. Microbiol. 2011; 79:133–148. [PubMed: 21166899]

15. Wolschendorf F, et al. Copper resistance is essential for virulence of *Mycobacterium tuberculosis*. Proc. Natl. Acad. Sci. USA. 2011; 108:1621–1626. [PubMed: 21205886]
16. Rowland JL, Niederweis M. Resistance mechanisms of *Mycobacterium tuberculosis* against phagosomal copper overload. Tuberculosis (Edinb). 2012; 92:202–210. [PubMed: 22361385]
17. Portmann R, Poulsen KR, Wimmer R, Solioz M. CopY-like copper inducible repressors are putative 'winged helix' proteins. Biometals. 2006; 19:61–70. [PubMed: 16502332]
18. Shafeeq S, et al. The *cop* operon is required for copper homeostasis and contributes to virulence in *Streptococcus pneumoniae*. Mol. Microbiol. 2011; 81:1255–1270. [PubMed: 21736642]
19. Kazmierczak KM, Wayne KJ, Rechtsteiner A, Winkler ME. Roles of*rel*(*Spn*) in stringent response, global regulation and virulence of serotype 2 *Streptococcus pneumoniae* D39. Mol. Microbiol. 2009; 72:590–611. [PubMed: 19426208]
20. Jacobsen FE, Kazmierczak KM, Lisher JP, Winkler ME, Giedroc DP. Interplay between manganese and zinc homeostasis in the human pathogen *Streptococcus pneumoniae*. Metallomics. 2011; 3:38–41. [PubMed: 21275153]
21. Hava DL, Camilli A. Large-scale identification of serotype 4 *Streptococcus pneumoniae* virulence factors. Mol. Microbiol. 2002; 45:1389–1406. [PubMed: 12207705]
22. Corbett D, Schuler S, Glenn S, Andrew PW, Cavet JS, Roberts IS. The combined actions of the copper-responsive repressor CsoR and copper-metallochaperone CopZ modulate CopA-mediated copper efflux in the intracellular pathogen. Listeria monocytogenes. Mol. Microbiol. 2011; 81:457–472. [PubMed: 21564342]
23. Badarau A, Dennison C. Copper trafficking mechanism of CXXC-containing domains: insight from the pH-dependence of their Cu(I) affinities. J. Am. Chem. Soc. 2011; 133:2983–2988. [PubMed: 21323310]
24. Pufahl RA, et al. Metal ion chaperone function of the soluble Cu(I) receptor Atx1. Science. 1997; 278:853–856. [PubMed: 9346482]
25. Arnesano F, et al. Characterization of the binding interface between the copper chaperone Atx1 and the first cytosolic domain of Ccc2 ATPase. J. Biol. Chem. 2001; 276:41365–41376. [PubMed: 11500502]
26. Banci L, Bertini I, Cantini F, Chasapis CT, Hadjiliadis N, Rosato A. A NMR study of the interaction of a three-domain construct of ATP7A with copper(I) and copper(I)-HAH1: the interplay of domains. J. Biol. Chem. 2005; 280:38259–38263. [PubMed: 16172131]
27. Banci L, Bertini I, Ciofi-Baffoni S, Kandias NG, Robinson NJ, Spyroulias GA, et al. The delivery of copper for thylakoid import observed by NMR. Proc. Natl. Acad. Sci. USA. 2006; 103:8320–8325. [PubMed: 16707580]
28. Banci L, Bertini I, Del Conte R, Markey J, Ruiz-Duenas FJ. Copper trafficking: the solution structure of *Bacillus subtilis* CopZ. Biochemistry. 2001; 40:15660–15668. [PubMed: 11747441]
29. Taylor AB, Stoj CS, Ziegler L, Kosman DJ, Hart PJ. The copper-iron connection in biology: structure of the metallo-oxidase Fet3p. Proc. Natl. Acad. Sci. USA. 2005; 102:15459–15464. [PubMed: 16230618]
30. Banci L, Bertini I, Ciofi-Baffoni S, Katsari E, Katsaros N, Kubicek K, et al. A copper(I) protein possibly involved in the assembly of CuA center of bacterial cytochrome c oxidase. Proc. Natl. Acad. Sci. USA. 2005; 102:3994–3999. [PubMed: 15753304]
31. Abriata LA, Banci L, Bertini I, Ciofi-Baffoni S, Gkazonis P, Spyroulias GA, et al. Mechanism of Cu(A) assembly. Nat. Chem. Biol. 2008; 4:599–601. [PubMed: 18758441]
32. Gourdon P, Liu XY, Skjorringe T, Morth JP, Moller LB, Pedersen BP, et al. Crystal structure of a copper-transporting PIB-type ATPase. Nature. 2011; 475:59–64. [PubMed: 21716286]
33. Rosenzweig AC. Copper delivery by metallochaperone proteins. Acc. Chem. Res. 2001; 34:119–128. [PubMed: 11263870]
34. Xiao Z, Brose J, Schimo S, Ackland SM, La Fontaine S, Wedd AG. Unification of the copper(I) binding affinities of the metallo-chaperones Atx1, Atox1, and related proteins: detection probes and affinity standards. J. Biol. Chem. 2011; 286:11047–11055. [PubMed: 21258123]
35. Dupont CL, Grass G, Rensing C. Copper toxicity and the origin of bacterial resistance--new insights and applications. Metallomics. 2011; 3:1109–1118. [PubMed: 21984219]

36. Rosenzweig AC. Metallochaperones: bind and deliver. Chem Biol. 2002; 9:673–677. [PubMed: 12079778]
37. Banci L, Bertini I, Ciofi-Baffoni S, Kozyreva T, Zovo K, Palumaa P. Affinity gradients drive copper to cellular destinations. Nature. 2010; 465:645–648. [PubMed: 20463663]
38. Badarau A, Dennison C. Thermodynamics of copper and zinc distribution in the cyanobacterium *Synechocystis* PCC 6803. Proc. Natl. Acad. Sci. USA. 2011; 108:13007–13012. [PubMed: 21778408]
39. Zaballa ME, Abriata LA, Donaire A, Vila AJ. Flexibility of the metal-binding region in apo-cupredoxins. Proc. Natl. Acad. Sci. USA. 2012; 109:9254–9259. [PubMed: 22645370]
40. Bersch B, Derfoufi KM, De Angelis F, Auquier V, Ekende EN, Mergeay M, et al. Structural and metal binding characterization of the C-terminal metallochaperone domain of membrane fusion protein SilB from *Cupriavidus metallidurans* CH34. Biochemistry. 2011; 50:2194–2204. [PubMed: 21299248]
41. Wu CC, Rice WJ, Stokes DL. Structure of a copper pump suggests a regulatory role for its metal-binding domain. Structure. 2008; 16:976–985. [PubMed: 18547529]
42. Gonzalez-Guerrero M, Arguello JM. Mechanism of Cu+-transporting ATPases: soluble Cu+ chaperones directly transfer Cu+ to transmembrane transport sites. Proc. Natl. Acad. Sci. USA. 2008; 105:5992–5997. [PubMed: 18417453]
43. Chillappagari S, Miethke M, Trip H, Kuipers OP, Marahiel MA. Copper acquisition is mediated by YcnJ and regulated by YcnK and CsoR in *Bacillus subtilis*. J. Bacteriol. 2009; 191:2362–2370. [PubMed: 19168619]
44. Ekici S, Yang H, Koch HG, Daldal F. Novel transporter required for biogenesis of cbb3-type cytochrome c oxidase in *Rhodobacter capsulatus*. MBio. 2012; 3:e00293–e00311. [PubMed: 22294680]
45. Ramos-Montanez S, Kazmierczak KM, Hentchel KL, Winkler ME. Instability of *ackA* (acetate kinase) mutations and their effects on acetyl phosphate and ATP amounts in *Streptococcus pneumoniae* D39. J. Bacteriol. 2010; 192:6390–6400. [PubMed: 20952579]
46. Anjem A, Imlay JA. Mononuclear iron enzymes are primary targets of hydrogen peroxide stress. J. Biol. Chem. 2012; 287:15544–15556. [PubMed: 22411989]
47. Lynch JP 3rd, Zhanel GG. *Streptococcus pneumoniae:* epidemiology and risk factors, evolution of antimicrobial resistance, and impact of vaccines. Curr. Opin. Pulm. Med. 2010; 16:217–225. [PubMed: 20375783]
48. Lanie JA, Ng WL, Kazmierczak KM, Andrzejewski TM, Davidsen TM, Wayne KJ, et al. Genome sequence of Avery's virulent serotype 2 strain D39 of *Streptococcus pneumoniae* and comparison with that of unencapsulated laboratory strain R6. J. Bacteriol. 2007; 189:38–51. [PubMed: 17041037]
49. Ramos-Montanez S, Tsui HC, Wayne KJ, Morris JL, Peters LE, Zhang F, et al. Polymorphism and regulation of the *spxB* (pyruvate oxidase) virulence factor gene by a CBS-HotDog domain protein (SpxR) in serotype 2 *Streptococcus pneumoniae*. Mol. Microbiol. 2008; 67:729–746. [PubMed: 18179423]
50. Wayne KJ, Sham LT, Tsui HC, Gutu AD, Barendt SM, Keen SK, et al. Localization and cellular amounts of the WalRKJ (VicRKX) two-component regulatory system proteins in serotype 2 *Streptococcus pneumoniae*. J. Bacteriol. 2010; 192:4388–4394. [PubMed: 20622066]
51. Kuzmic P. Program DYNAFIT for the analysis of enzyme kinetic data: application to HIV proteinase. Anal. Biochem. 1996; 237:260–273. [PubMed: 8660575]
52. Adams PD, Afonine PV, Bunkoczi G, Chen VB, Davis IW, Echols N, et al. PHENIX: a comprehensive Python-based system for macromolecular structure solution. Acta Crystallogr. D. 2010; 66:213–221. [PubMed: 20124702]
53. Emsley P, Cowtan K. Coot: model-building tools for molecular graphics. Acta Crystallogr. D. 2004; 60:2126–2132. [PubMed: 15572765]
54. Delaglio F, Grzesiek S, Vuister GW, Zhu G, Pfeifer J, Bax A. NMRPipe: a multidimensional spectral processing system based on UNIX pipes. J. Biomol. NMR. 1995; 6:277–293. [PubMed: 8520220]

55. Lescop E, Rasia R, Brutscher B. Hadamard amino-acid-type edited NMR experiment for fast protein resonance assignment. J. Am. Chem. Soc. 2008; 130:5014–5015. [PubMed: 18345629]

56. Lescop E, Schanda P, Brutscher B. A set of BEST triple-resonance experiments for time-optimized protein resonance assignment. J. Magn. Reson. 2007; 187:163–169. [PubMed: 17468025]

57. Webb SM. SIXpack: a graphical user interface for XAS analysis using IFEFFIT. Physica Scripta. 2005; T115:1011–1014.

58. Zabinsky SI, Rehr JJ, Ankudinov A, Albers RC, Eller MJ. Multiplescattering calculations of x-ray-absorption spectra. Phys. Rev. B. 1995; 52:2995–3009.

59. Ankudinov AL, Ravel B, Rehr JJ, Conradson SD. Real-space multiplescattering calculation and interpretation of x-ray-absorption near-edge structure. Phys Rev B. 1998; 58:7565–7576.

60. Leitch S, Bradley MJ, Rowe JL, Chivers PT, Maroney MJ. Nickel-specific response in the transcriptional regulator, *Escherichia coli* NikR. J. Am. Chem. Soc. 2007; 129:5085–5095. [PubMed: 17397155]

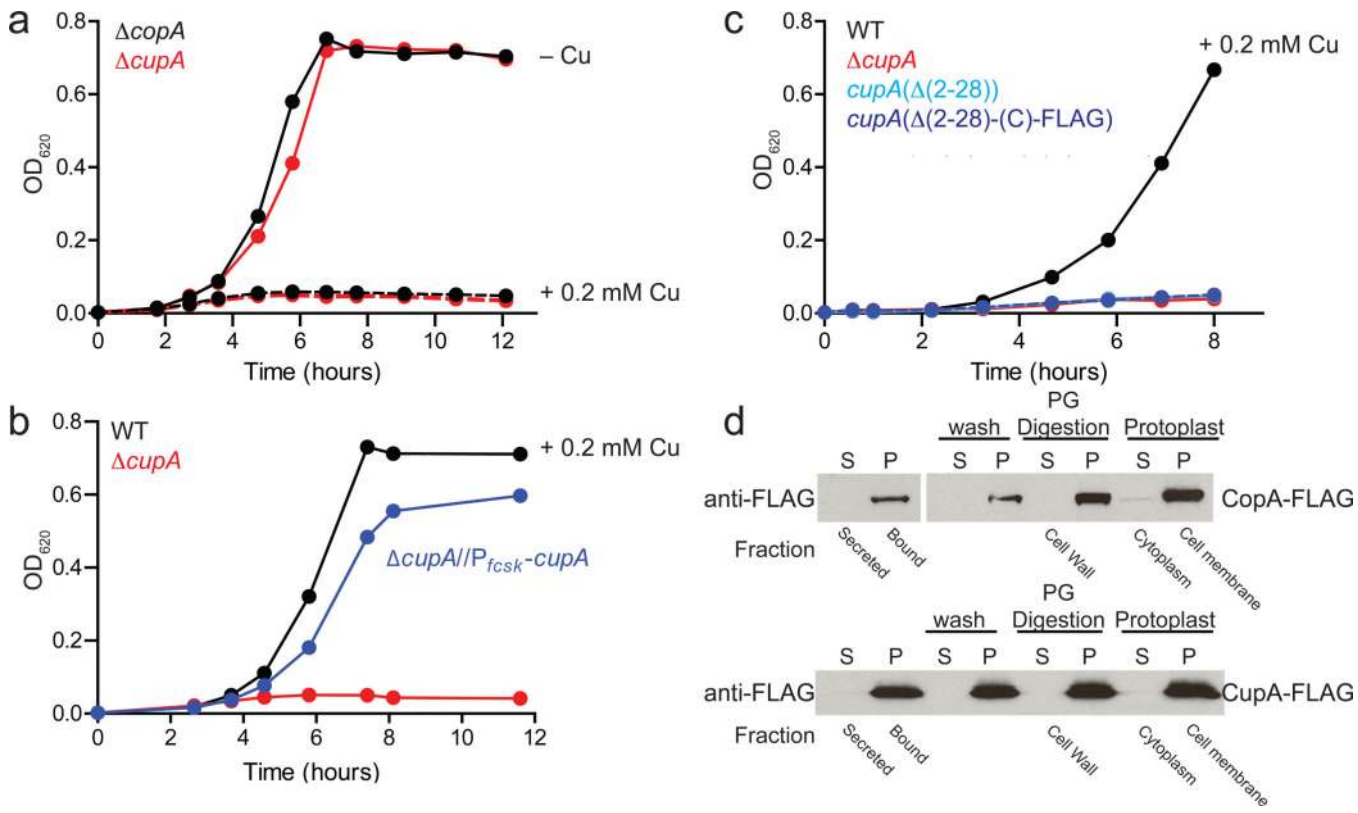

Figure 1. Copper sensitivity phenotypes of mutant *S. pneumoniae* D39 strains

Δ*cupA* and Δ*copA Spn* strains are highly sensitive to copper toxicity (**a**) which can be reversed by expression of *cupA* from a heterologous promoter (**b**). (**c**) Deletion of the single putative transmembrane helix abrogates copper resistance to an extent comparable to inactivation of CopA(D442A) (compare to Supplementary Fig. 4d). In all cases, two independent isolates of the same strain designation were constructed and duplicate (or more) growth experiments were carried out with each of the two strains. (**d**) Both CopA and CupA localize to the cell membrane fraction. The results of a subcellular fractionation of *copA*-(C)-FLAG (IU6044) (top) and *cupA*-(C)-FLAG (IU6041) (bottom) with visualization by anti-FLAG western blotting. Supernatants (S) or pellets (P) are marked for centrifugation steps, and cell fractions are indicated below the blots. See Supplementary Figure 6 for additional experimental details and the full blot and Supplementary Tables 1 and 2 for strain details.

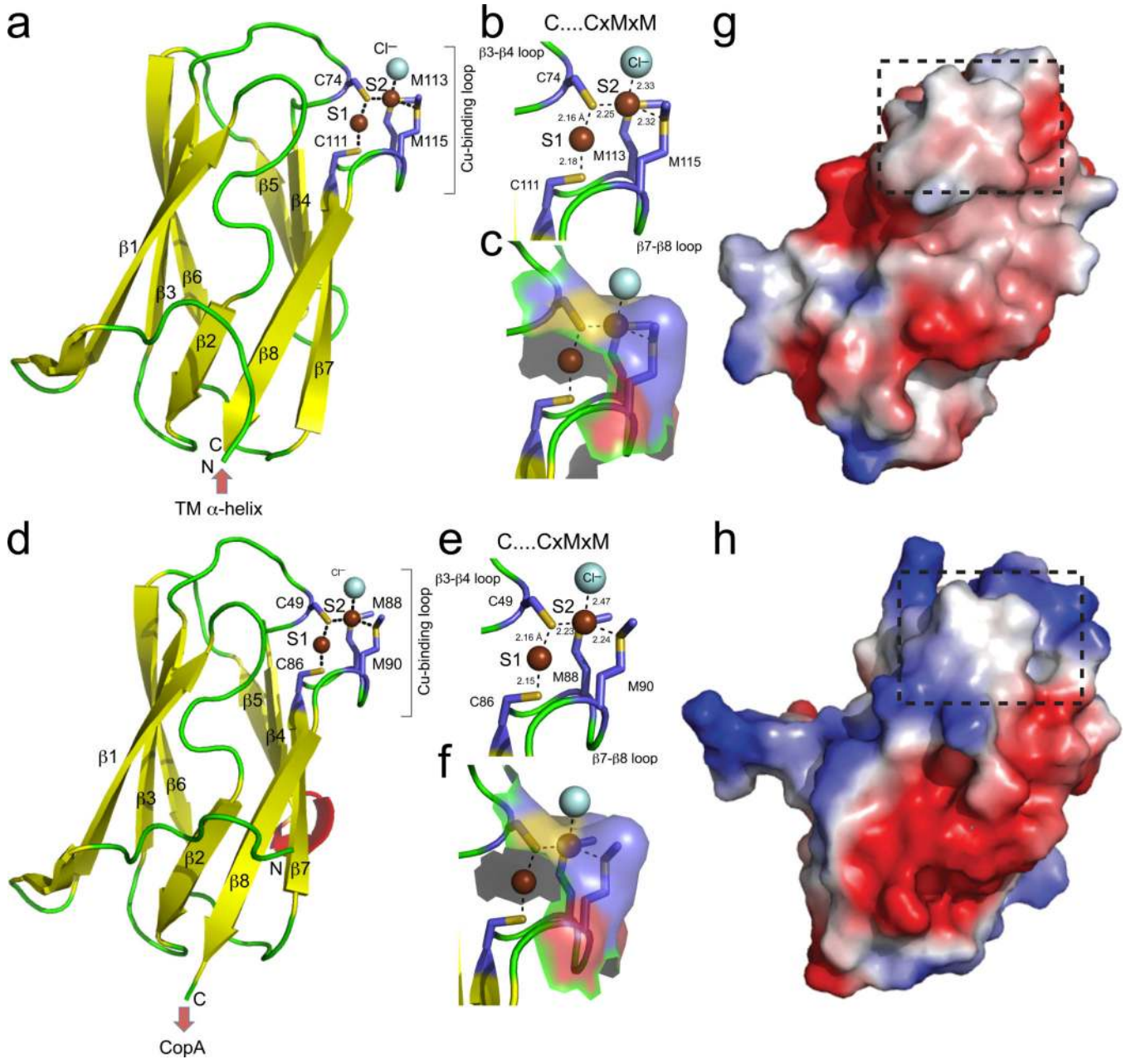

Figure 2. Crystallographic structures of sCupA and CopA^{MBD}

Structure representations of sCupA (**a–c**) and CopA^{MBD} (**d–f**). Close-up views of the Cu(I) coordination geometries of each protein are shown (**b, e**) as are solvent-accessible surface areas (arbitrarily colored according to residue type) (**c, f**) around each binuclear Cu(I) chelate. Electrostatic surface potentials (painted based on surface potentials) of sCupA (**g**) and CopA^{MBD} (**h**). Structure statistics compiled in Supplementary Table 3.

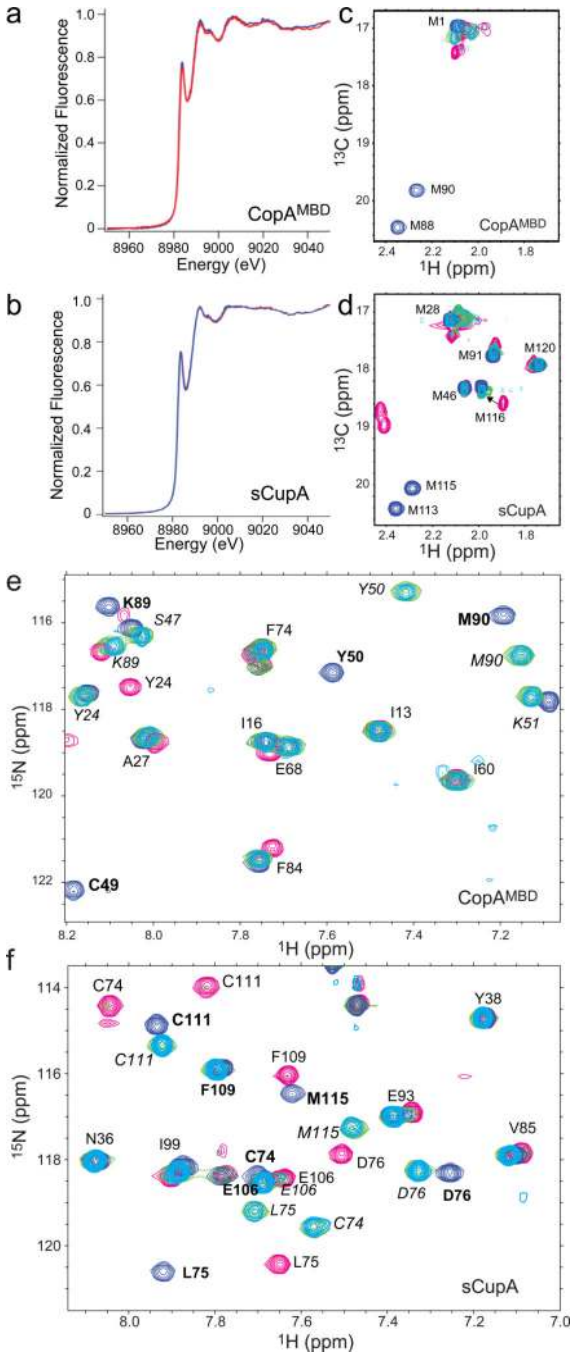

Figure 3. The Met-rich S2 site is the low-affinity site on both CopA^{MBD} and sCupA and Cu(I) is transferred only from the S2 site of sCupA to the S1 site of apo-MBD

X-ray absorption near-edge spectra (XANES) of Cu_1 CopA^{MBD} (**a**) and Cu_1 sCupA (**b**) in the presence of 0.2 M NaBr (red) or 0.2 M NaCl (blue). Overlay of the Met thioether methyl ($^{13}C\varepsilon$-$^{1}H\varepsilon$) region of an ^{1}H,^{13}C-HSQC spectrum for CopA^{MBD} (**c**) and sCupA (**d**) acquired in the apo-state (magenta), Cu_1 state (green) and Cu_2 states (blue). Cyan crosspeaks result when apo-MBD is mixed with 2.0 mol equiv of Cu_2 sCupA (**c**) or 1.0 mol equiv of Cu_2

sCupA (**d**). Overlay of the backbone $^{1}H,^{15}N$-HSQC spectra of $CopA^{MBD}$ (**e**) and sCupA (**f**), with the same crosspeak color pattern as in panels **c,d**.

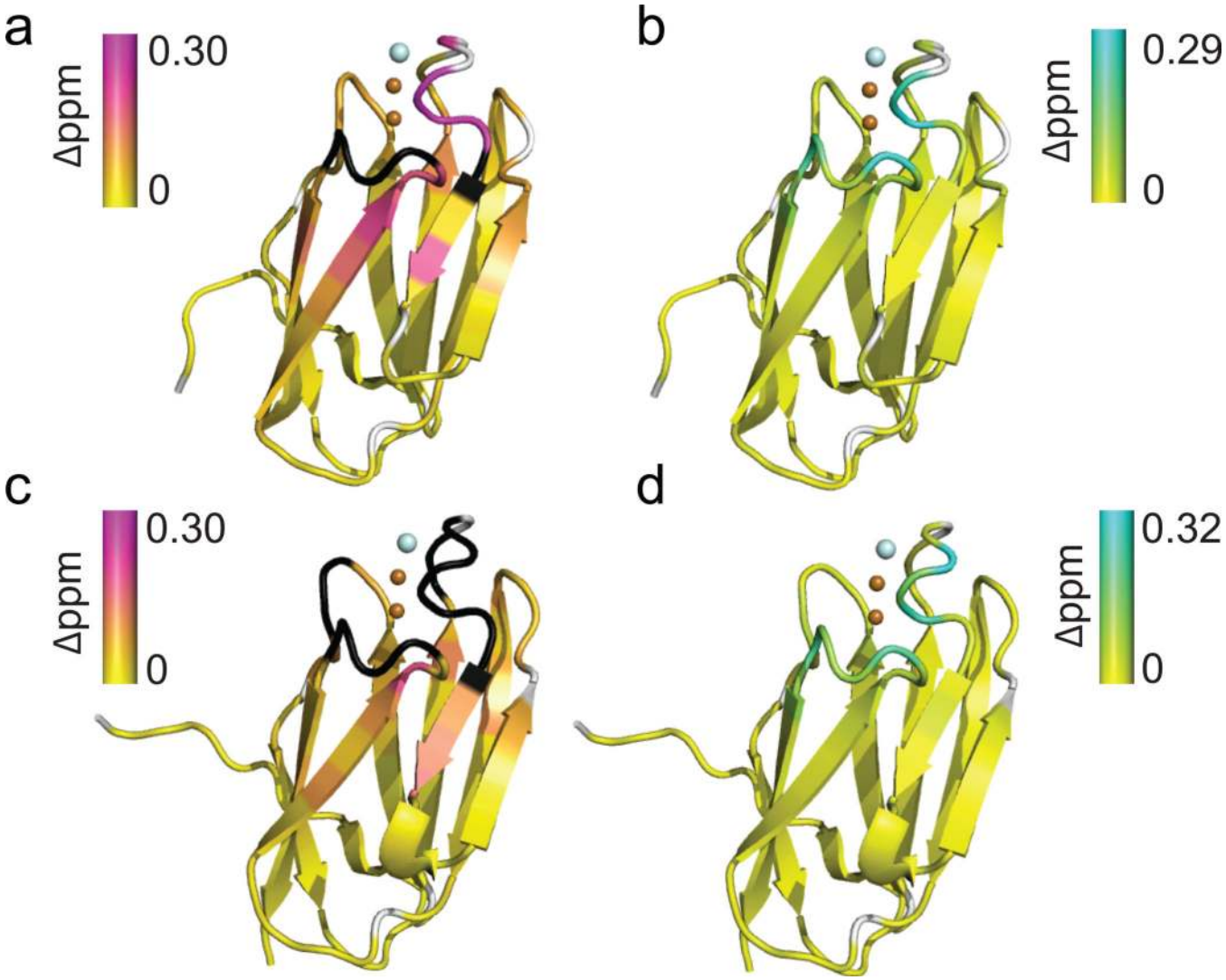

Figure 4. NMR chemical shift perturbation analysis of sCupA and CopA^{MBD} induced by Cu(I) binding

Ribbon representation of the changes in backbone amide chemical shift upon Cu(I) binding by sCupA (**a,b**) and CopA^{MBD} (**c,d**). Panels **a** and **c** represent Δppm (Cu_1–apo) while panels **b** and **d** represent Δppm (Cu_2–Cu_1). The ribbon is painted white for Pro residues and black for those resonances broadened beyond detection in the apo-state in each case.

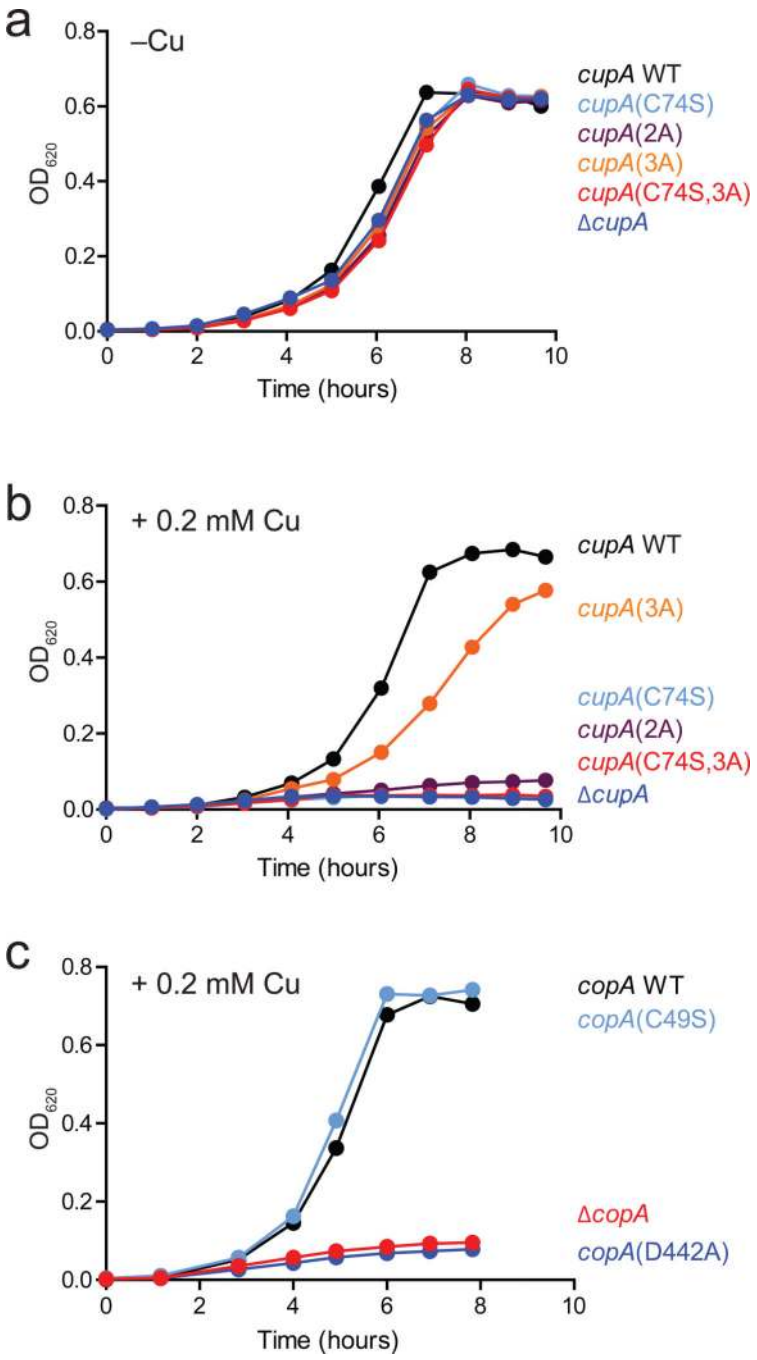

Figure 5. Mutagenesis of CupA Cu(I) binding residues partly or completely abrogates Cu(I) resistance by *S. pneumoniae*, but not in CopA^{MBD}

Representative growth curves for the indicated *S. pneumoniae* strains in BHI in the absence (**a**) or presence (**b,c**) of 0.2 mM Cu(II) added to the growth medium. In all cases, two independent isolates of the same strain designation were constructed and duplicate (or more) growth experiments were carried out with each of the two strains. See Supplementary Tables 1 and 2 for strain details.

Table 1

Cu(I) binding affinities for sCupA and $CopA^{MBD}$

Protein	log K_{Cu1} (M^{-1})	log K_{Cu2} (M^{-1})	log $\beta_{2,Cu}$ (M^{-2})
sCupA	17.9 (±0.3)	14.8 (±0.2)[2]	32.6 (±0.3)
$CopA^{MBD}$	16.3 (±0.1)	13.4 (±0.3)	29.8 (±0.3)

Parameters (mean values ± s.d.) were measured via global analysis of multiple anaerobic CuCl titrations using BCA or BCS as a competitor Cu chelator (Supplementary Figs. 7–9) using a nonlinear least squares fit to a stepwise two-Cu(I) binding model in both cases.

[2]Mean value from BCA and BCS titrations. Conditions: 25 mM Hepes, 0.2 M NaCl, pH 7.0, 22 °C.